

The expression of transporter OATP2/OATP8 decreases in undetectable hepatocellular carcinoma by Gd-EOB-MRI in the explanted cirrhotic liver

A short title: OATP expression in undetected HCC

Masaaki Hidaka¹⁾, Mitsuhsa Takatsuki¹⁾, Sadayuki Okudaira¹⁾, Akihiko Soyama¹⁾, Izumi Muraoka¹⁾,
Takayuki Tanaka¹⁾, Izumi Yamaguchi¹⁾, Takanobu Hara¹⁾, Hisamitsu Miyaaki²⁾, Tatsuki Ichikawa²⁾,
Tomayoshi Hayashi³⁾, Ichiro Sakamoto⁴⁾, Kazuhiko Nakao²⁾, Tamotsu Kuroki¹⁾, Takashi Kanematsu¹⁾,
Susumu Eguchi¹⁾

1) Department of Surgery, Nagasaki University Graduate School of Biomedical Sciences, Nagasaki,
Japan

2) Department of Gastroenterology and Hepatology, Nagasaki University Graduate School of
Biomedical Sciences, Nagasaki Japan

3) Department of Pathology, Nagasaki University Hospital, Nagasaki, Japan.

4) Department of Radiological Sciences, Nagasaki University Graduate School of Biomedical
Sciences, Nagasaki Japan

Keywords: hepatocellular carcinoma, EOB-MRI, OATP, transporter,

Address correspondence to: Susumu Eguchi, M.D., Ph.D.

Department of Surgery, Nagasaki University Graduate School of Biomedical Sciences, 1-7-1

Sakamoto, Nagasaki 852-8501, Japan

TEL:+ 81-95-819-7316 FAX: +81-95-819-7319

E-mail: sueguchi@nagasaki-u.ac.jp

Number of words in manuscript: 2434

Number of figures and tables: 3 figures, 2 tables

Abbreviations: hepatocellular carcinoma (HCC), Gadoteric acid-enhanced magnetic resonance imaging (Gd-EOB-MRI), multi-detector computed tomography (MD-CT), organic anion transporter (OATP), model for end-stage liver disease (MELD), alpha-fetoprotein(AFP), protein induced by Vitamin K absence or antagonists-II (PIVKAI), radio frequency ablation (RFA), trans-arterial chemoembolization (TACE), multidrug-resistant protein (MRP),

Conflict of interest: no conflict of interest

Financial support: no grant and no the other financial grant support

Abstract

Purpose: The aim of this study is to evaluate the detectability of hepatocellular carcinoma (HCC) in the explanted cirrhotic liver using Gadoteric acid-enhanced magnetic resonance imaging (Gd-EOB-MRI) and the degree of organic anion transporter OATP2/OATP8 (OATP1B1/1B3) HCC which couldn't be preoperatively detected by multi-detector computed tomography (MD-CT) and Gd-EOB-MRI.

Methods: Eleven patients (HBV 3, HCV 7, nonBnonC 1) out of 145 recipients of liver transplantation were analyzed. The detectability by each imaging modality and the expression of OATP2/OATP8 of HCC were analyzed using the whole liver thin sliced histological and immunohistochemical examination retrospectively. **Results:** The imaging examination detected 17 lesions of HCC by MDCT and/or Gd-EOB-MRI. Only one lesion detected by Gd-EOB-MRI had well differentiated and minute (7mm) HCC. However, the histological examination revealed newly 11 lesions and one false-positive lesion of HCC in the explanted livers. The median diameter of the preoperatively undetectable HCC by imaging was 8 mm (2-12). The histological characteristic of the preoperatively undetectable HCC was well differentiated HCC (10/11). The accuracy rate in MDCT and Gd-EOB-MRI was 53.6% (15/28) and 57.1% (16/28). The rate of positive predictive value in MDCT and Gd-EOB-MRI was 93.7% (15/16) and 94.2%

(16/17) respectively. The expression of OATP2/OATP8 in the preoperatively undetectable HCC was negative in 9 lesions, was weak positive in 2 lesions.

Conclusions: The detectability of Gd-EOB-MRI is almost equal to MDCT in a cirrhotic liver. Small HCCs were difficult to detect even with Gd-EOB-MRI. The transporter of OATP2/OATP8 was less expressed in the preoperatively undetectable HCCs.

Keywords: hepatocellular carcinoma, EOB-MRI, transporter, OATP

1 INTRODUCTION

2 Hepatocellular carcinoma (HCC) is the seventh most common cancer in
3 patients with chronic liver disease particularly with hepatitis B and C virus related
4 hepatic dysfunction such as liver cirrhosis in the world [1]. Early and adequate
5 diagnosis of HCC in the patient underlying liver dysfunction by optimal imaging
6 modalities is likely to contribute to select the treatment and management for HCC and
7 affect the mortality after various treatments which are the resection, liver transplantation,
8 radio frequency ablation (RFA) and trans-arterial chemoembolization (TACE) [2-5]. A
9 guideline from the American Association for the Study of Liver diseases has
10 recommended that nodules with 1-2cm in diameter in a cirrhotic liver should be
11 investigated with 2 dynamic studies, including either computed tomography (CT) scan,
12 contrast ultrasound or magnetic resonance imaging (MRI) [4,6]. In recent years, liver
13 specific agent has improved the detection of liver tumors.
14 Gadoxetate-ethoxybenzyl-diethylenetriamine (Gd-EOB-DTPA; Primovist, Bayer
15 Schering Pharma AG, Berlin, Germany) have been used as the liver specific contrast
16 agent for detection of HCC [7]. This agent is initially taken up by hepatocytes and
17 excreted to the biliary system. In a rodent study, the gadoxetic acid was uptaken by
18 organic anion-transporting polypeptide (OATP) 2/8 (OATP1B1/1B3) and the excreted to

1 the biliary canaliculi through the export transporter, multidrug-resistant protein (MRP) 2
2 [8, 9]. Several reports indicated that the expression of hepatocyte transporter especially
3 OATP2/OATP8 in HCC correlated with the enhancement of Gd-EOB-MRI in the
4 hepatocyte phase [10-12].

5 Compared with MD-CT, some investigators indicated that Gd-EOB-MRI had
6 significantly higher accuracy and sensitivity in the detection of small HCC in patients
7 with normal liver and liver cirrhosis [13-15].

8 However we have reported that there are some HCCs in the explanted cirrhotic liver in
9 the liver transplantation which could not be detected by even current modalities [16]. It
10 is uncertain about the degree of the expression in an undetectable HCC by the advanced
11 modalities including GD-EOB-MRI and the real detectability of HCC in the cirrhotic
12 explanted liver.

13 This study aims to reveal the real detectability of MD-CT and Gd-EOB-MRI and
14 the expression of hepatocyte transporter of HCC in the explanted cirrhotic liver which
15 could not be detected preoperatively even by Gd-EOB-MRI.

16

17 **METHODS**

18 **Patients**

1 We had 146 cases in liver transplantation (LT) in our university from 1997 to
2 July 2011. Between 2008 and 2010, eleven patients (HBV 3, HCV 7, nonBnonC 1)
3 out of 145 cases of LDLT were analyzed. From 2008 Gd-EOB-MRI had been used for
4 the diagnosis of all patients with HCC before LT. MD-CT and Gd-EOB-MRI was done
5 to evaluate the status of HCC. Our policy of the indication of LDLT for the patients with
6 HCC stick to the Milan Criteria: solitary tumor less than 5 cm, multiple tumor less than
7 3 nodules and 3 cm (17, 18). The details of these patients were described as follows,
8 Backgrounds of the patients were Child-Pugh score 9 (median, 6-13), MELD score 11.5
9 (7-16), AFP 9.6 ng/ml (3.2-506), and PIVKA-II 38mAU/ml (10-80) respectively in
10 Table 1.

11

12 **Imaging and diagnostic methods**

13 **Multidetector CT technique**

14 CT was performed with a 64-MDCT scanner (Aquilion 64, Toshiba Medical
15 Systems) with the following scanning parameters: rotation time, 0.5 second; beam
16 collimation, 64 × 0.5 mm; section thickness and interval, 3 mm and 2.4mm; field of
17 view, 32 cm;120 kV; tube current, 250–350 mAs. All helical scans were started from
18 the top of the liver and proceeded in a cephalocaudal direction. In each patient,

1 unenhanced and three-phase (arterial, portal, and delayed phase) contrast-enhanced
2 helical scans of the whole liver were obtained. Patients were instructed to hold their
3 breath during scanning. A dose of 110 – 135ml of nonionic contrast material (iomeprol;
4 Iomeron, Bracco) was injected into an antecubital vein at a rate of 4- 5 mL/s. An
5 automatic bolus tracking program (Real Prep, Toshiba Medical Systems) was used to
6 time the start of acquisition after contrast injection.

7

8 **MR imaging technique**

9 MR imaging was performed with a 1.5T superconducting system (Signa, GE
10 Medical Systems, Milwaukee, WI, USA), using a body phased array multicoil for signal
11 detection. Unenhanced sequences included breath-hold T2-weighted single-shot FSE
12 sequences with and without fat saturation, and breath-hold T1-weighted GRE dual-echo
13 “in and out of phase”. Contrast-enhanced sequences were acquired after intravenous
14 injection of Gd-EOB-DTPA at a dose of 0.1 ml/kg body weight at a speed of 1.5 ml/sec
15 immediately followed by a 20-mL saline flush, using a dual power injector. Both
16 dynamic and hepatobiliary-phase images were obtained using a fat-suppressed, 3D GRE
17 sequence (Liver Acquisition with Volume Acceleration: LAVA, GE Medical Systems)
18 before and after IV bolus administration of Gd-EOB-DTPA. Imaging delay times were

1 determined with an automatic bolus tracking program (Smart Prep, GE Medical
2 Systems) after contrast agent administration. Hepatic arterial phase images were
3 obtained 10 s after the arrival of contrast medium in the proximal abdominal aorta, and
4 portal venous and equilibrium phase images were obtained, respectively, 60 and 180 s
5 after the beginning of the injection. Finally, hepatobiliary-phase imaging was obtained
6 20 min after the beginning of contrast-medium injection.

7

8 **Diagnosis of HCC by imaging**

9 Images were diagnosed by experienced radiologist before LT. Criteria for the
10 diagnosis of HCC was shown as follows. HCC was diagnosed if two imaging
11 characteristics were met: (a) the nodule was seen to clearly enhance during the hepatic
12 arterial phase in MD-CT, Gd-EOB-MRI or (b) the nodule had washout during portal
13 venous phase in MD-CT, had hypointence to the surrounding liver during the
14 hepatobiliary phase.

15

16 **Histopathologic analysis**

17 The detectability in each imaging modality was analyzed using the whole liver
18 thin sliced histological examination [16]. Explanted livers were fixed in 10% formalin

1 for 48 hours. The livers were then sectioned and serial sections were cut from paraffin
2 blocks. Each section carefully was made from the paraffin-embedded blocks and stained
3 with hematoxylin and eosin. Suspicious nodules by gross inspection were examined
4 by an experienced pathologist (co-author S.O. T.H.). The pathological
5 diagnoses and analyses were made according to the third edition of *The*
6 *General Rules for the Clinical and Pathological Study of Primary Liver*
7 *Cancer*, published by the Liver Cancer Study Group of Japan (LCSGJ) and
8 Consensus for small hepatocellular carcinoma [19].

9 Immunohistochemical examination was performed as follows. Sections were
10 deparaffinized by ethanol concentrations and washed in tris-phosphate-buffered saline
11 (TBS). Then, the sections in pH 6.0 citric acid buffer solution were treated with
12 microwave at 125 °C for antigen retrieval for 10 min.

13 After washing, they were treated with 0.1% H₂O₂ at room temperature for 10min. The
14 sections were reacted at room temperature for 60 min with primary monoclonal
15 antibodies against OATP2/OATP8 (OATP1B1/1B3) (1:30) (Cat. No. 651140, Progen
16 Biotechnik, Heidelberg, Germany). Secondary antibody (EnvisionTM; DAKO, Chicago,
17 USA) was used at room temperature for 30 min. The sections were stained with 3,
18 3-diaminobenzidine tetrahydrochloride (DAB) for visualization. The sections were

1 counterstained with Mayer's Hematoxylin.

2

3 **Statistical Analysis**

4 The diagnostic accuracy, sensitivity, and positive predictive value of MD-CT
5 and Gd-EOB-MRI in the diagnosis of HCC were evaluated all lesions. The suspicious
6 lesions were assessed and measured by a radiologist. The macroscopic lesions of HCC
7 were assessed and measured by a pathologist in each section. In this retrospective
8 analysis, the accuracy of diagnosis was calculated as the real number of HCCs in the
9 whole explanted liver examination and number of true negative lesions divided by
10 number of HCCs and false-positive, false-negative lesions and true-negative lesions
11 (16). Sensitivity was calculated as the number of true-positive lesions divided by the
12 total number of HCCs. Positive predictive value was calculated as the number of HCCs
13 divided by the number of HCCs and the number of false-positive lesions. A chi-square
14 test was used in the differences of accuracy, sensitivity and positive predictive value
15 between MD-CT and Gd-EOB-MRI. Significance level was considered statistically
16 significant when the p-values were less than 0.05. Statistical analysis was done by SPSS
17 Version 18.0.

18

1 **RESULTS**

2 **Accuracy, Sensitivity and Positive predictive value**

3 Preoperative evaluation of HCC in the patients with LC detected 17 lesions in
4 11 patients by MD-CT and/or Gd-EOB-MRI, however, one nodule was only detected by
5 Gd-EOB-MRI before LT. The histological whole liver examination revealed newly 11
6 lesions of HCC and one false positive lesion in the explanted livers. A total of HCC in
7 the explanted liver was 28 nodules.

8 In comparison of the diagnostic accuracy, sensitivity and positive predictive
9 value of HCC in MDCT and Gd-EOB-MRI, all parameters were greater with
10 Gd-EOB-MRI than MDCT (Accuracy Gd-EOB-MRI vs. MDCT: 57.1% (16/28) vs.
11 53.5% (15/28), Sensitivity: 59.2% (16/27) vs. 55.5% (15/27) and Positive predictive
12 value: 94.1% (16/17) vs. 88.2% (15/17)), respectively in Table 1. The HCC only
13 detected by Gd-EOB-MRI was hypervascular nodule at arterial phase, iso-intence
14 nodule at hepatobiliary phase, 8 mm in a diameter and well differentiated tumor in the
15 pathological finding.

16

17 **Pathological comparison of preoperatively detected and undetected HCC**

18 A total of 17 lesions were detected by Gd-EOB-MRI and/or MDCT. Eleven

1 hypervascular nodules and 8 hypovascular nodules were detected by MDCT. Thirteen
2 hypervascular nodules and 11 hypointense nodules at the hepatocyte phase were
3 detected by Gd-EOB-MRI.

4 The mean tumor diameter of preoperatively undetectable HCC was
5 significantly smaller than detected HCC (undetectable HCC: mean diameter 0.8 cm,
6 range 0.2 – 1.1 cm vs. detectable HCC: 1.85 cm, range 0.7 – 4.2 cm, $p < 0.001$).
7 However, the differentiation of these tumors was similar (undetectable HCC: 13 well, 3
8 moderate vs. detectable HCC: 9 well, 2 moderate, $p=0.97$) in Table 2.

9

10 **The expression of OATP2/OATP8 in the undetectable HCCs by Gd-EOB-MRI**

11 The characteristics and expression of OATP2/OATP8 in the undetectable HCC
12 by Gd-EOB-MRI was shown in the Table 2. The no expression of OATP2/OATP8 in
13 HCC and the expression of OATP2/OATP8 in liver parenchyma with liver cirrhosis are
14 shown in Fig 1. The negative and weak expression of OATP2/OATP8 in the
15 undetectable HCC was shown in Fig 2. Nine lesions of the undetectable HCC had the
16 negative of the expression of OATP2/OATP8, weak expression was shown in 2 lesions.

17

18 **DISCUSSION**

1 Some reports indicated that the detectability of HCC was significantly higher in
2 the Gd-EOB- MRI than MD-CT in the normal liver and even though in cirrhotic liver
3 [13-15]. The results of this study revealed that there were HCCs in the cirrhotic liver
4 which can not be detected preoperatively by even Gd-EOB-MRI although the accuracy
5 of Gd-EOB-MRI was superior to MD-CT. These data was based on the weakness of
6 contrast in the hepatic phase by Gd-EOB-MRI as the uptake of the contrast agent in the
7 cirrhotic liver was decreased [19, 20]. Usually the border between HCC lesion and
8 normal liver was identified clearly in the hepatic phase however the image contrast in
9 the cirrhotic liver was not clear in the border between the malignant lesion and the
10 normal liver. Di Martino et al reported that the detectability of HCC less than 2 cm by
11 Gd-EOB-MRI was significantly higher than MDCT [15]. Mita et al indicated that there
12 was no difference between Gd-EOB-MRI, Sonazoid contrast-enhanced ultrasonography
13 and CT arterioportal angiography for diagnosing HCC in nodules smaller than 2 cm.
14 [21]. Tajima et al reported that the degree of liver enhancement was significantly lower
15 in the chronic liver dysfunction than the normal liver function group. The cirrhotic liver
16 has the potential of multi-centric carcinogenesis and the minute HCC which we had
17 reported before [16]. The characteristic of undetectable HCC was minute nodule smaller
18 than 1 cm (median diameter: 8 mm) in our results. These finding might be associated

1 that the contrast enhancement between HCC and the cirrhotic liver was not clear in the
2 hepatobiliary phase. Even though the modalities of the image have been progressed, it
3 was difficult to detect the minute HCC in the cirrhotic liver by even Gd-EOB-MRI
4 because our patient was the end staged liver with high Child-Pugh score and MELD
5 score.

6 Recent studies investigated whether the transporter of Gd-EOB-MRI was
7 expressed in the HCC with various types. There was some HCC which had high
8 intensity of hepatocyte phase in Gd-EOB-MRI even with the expression of OATP
9 transporter [10]. These lesions were so called green hepatoma. They indicated the
10 degree of contrast in the hepatic phase has been increased as the OATP1B3 has been
11 more expressed in the HCC lesion. Our study revealed that the minute HCC in the
12 explanted liver which has not been detected even by Gd-EOB-MRI had no and less
13 expression of OATP2/OATP8. These findings might indicate the loss of membrane
14 transporter in the normal hepatocyte during the process of the carcinogenesis of HCC.
15 The transporter of the membrane of hepatocyte in the dysplastic nodule has been
16 maintained, thereafter has been lost the function of the membrane during the
17 carcinogenesis. However, in some cases the expression of OATP2/OATP8 in the
18 moderate HCC has acquired the expression of transporter in such as the green hepatoma.

1 It might be associated between the excretion of the transporter such as the multi
2 resistance drug protein which has the excretion part of the Gd-EOB-MRI into the bile
3 duct and bile canal. As the tumor has increased gradually to the moderate differentiation,
4 the failure and compression of the bile duct in HCC has done. The early HCC may have
5 lost the expression of the OATP2/OATP8 function on the membrane of carcinogenic
6 hepatocyte at first with the multi step carcinogenesis. Kitao et al reported that the
7 expression of OATP8 significantly decreases during multistep hepatocarcinogenesis
8 [23]. The less expression of OATP2/OATP8 has the potential biomarker of early HCC
9 such as Glypican 3 and Heat shock protein (HSP) 70 [24, 25].

10

11 **CONCLUSION**

12 The detectability of HCC by Gd-EOB-MRI is almost equal to MDCT in a
13 cirrhotic liver. Small HCCs were difficult to detect even with Gd-EOB-MRI. The
14 transporter of OATP2/OATP8 was less expressed in the preoperatively undetectable
15 HCCs.

16

1 **References**

- 2 1. Yang JD, Robert LR. Hepatocellular carcinoma: A global view. *Nat Rev*
3 *Gastroenterol Hepatol* 2010; 7: 448-458.
- 4 2. Bruix J, Sherman M. Management of Hepatocellular carcinoma: An update:
5 *Hepatology* 2011; 53: 1020-1022.
- 6 3. Bruix J, Sherman M. Management of Hepatocellular carcinoma. *Hepatology* 2005;
7 42: 1208-1236.
- 8 4. Aii S, Sata M, Sakamoto M, Shimada M, Kumada T, Shiina S, Kumada T, Shiina S,
9 Yamashita T, Kokudo N, Tanaka M, Takayama T, Kudo M. Management of
10 hepatocellular carcinoma: Report of Consensus Meeting in the 45th Annual Meeting
11 of the Japan Society of Hepatology (2009). *Hepatol Res* 2010; 40: 667-685.
- 12 5. Minami Y, Kudo M. Radiofrequency ablation of hepatocellular carcinoma: Current
13 status. *World J Radiol.* 2010; 28: 417-424.
- 14 6. Forner A, Vilana R, Ayuso C, Bianchi L, Solé M, Ayuso JR, Boix L, Sala M, Varela
15 M, Llovet JM, Brú C, Bruix J. Diagnosis of hepatic nodules 20 mm or smaller in
16 cirrhosis: Prospective validation of the noninvasive diagnostic criteria for
17 hepatocellular carcinoma. *Hepatology* 2008; 47:97-104.
- 18 7. Kim MJ. Current limitations and potential breakthroughs for the early diagnosis of

- 1 hepatocellular carcinoma. *Gut Liver* 2011; 5:15-21.
- 2 8. van Montfoort JE, Stieger B, Meijer DK, Weinmann HJ, Meier PJ, Fattinger KE.
3 Hepatic uptake of the magnetic resonance imaging contrast agent gadoxetate by the
4 organic anion transporting polypeptide Oatp1. *J Pharmacol Exp Ther.* 1999;
5 290:153-157.
- 6 9. Lorusso V, Pascolo L, Ferneti C, Visigalli M, Anelli P, Tiribelli C. In vitro and in
7 vivo hepatic transport of the magnetic resonance imaging contrast agent B22956/1:
8 role of MRP proteins. *Biochem Biophys Res Commun.* 2002; 293:100-105.
- 9 10. Narita M, Hatano E, Arizono S, Miyagawa-Hayashino A, Isoda H, Kitamura K,
10 Taura K, Yasuchika K, Nitta T, Ikai I, Uemoto S. Expression of OATP1B3
11 determines uptake of Gd-EOB-DTPA in hepatocellular carcinoma. *J Gastroenterol*
12 2009; 44:93-798.
- 13 11. Tsuboyama T, Onishi H, Kim T, Akita H, Hori M, Tatsumi M, Nakamoto A, Nagano
14 H, Matsuura N, Wakasa K, Tomoda K. Hepatocellular carcinoma:
15 hepatocyte-selective enhancement at gadoxetic acid-enhanced MR
16 imaging--correlation with expression of sinusoidal and canalicular transporters and
17 bile accumulation. *Radiology.* 2010; 255:824-33.
- 18 12. Kitao A, Zen Y, Matsui O, Gabata T, Kobayashi S, Koda W, Kozaka K, Yoneda N,

- 1 Yamashita T, Kaneko S, Nakanuma Y. Hepatocellular carcinoma: signal intensity at
2 gadoxetic acid-enhanced MR Imaging--correlation with molecular transporters and
3 histopathologic features. *Radiology*. 2010; 256:817-26.
- 4 13. Ichikawa T, Saito K, Yoshioka N, Tanimoto A, Gokan T, Takehara Y, Kamura T,
5 Gabata T, Murakami T, Ito K, Hirohashi S, Nishie A, Saito Y, Onaya H, Kuwatsuru
6 R, Morimoto A, Ueda K, Kurauchi M, Breuer J. Detection and characterization of
7 focal liver lesions: a Japanese phase III, multicenter comparison between gadoxetic
8 acid disodium-enhanced magnetic resonance imaging and contrast-enhanced
9 computed tomography predominantly in patients with hepatocellular carcinoma and
10 chronic liver disease. *Invest Radiol*. 2010; 45:133-41.
- 11 14. Kim SH, Kim SH, Lee J, Kim MJ, Jeon YH, Park Y, Choi D, Lee WJ, Lim HK.
12 Gadoxetic acid-enhanced MRI versus triple-phase MDCT for the preoperative
13 detection of hepatocellular carcinoma. *AJR Am J Roentgenol*. 2009; 192:1675-81.
- 14 15. Di Martino M, Marin D, Guerrisi A, Baski M, Galati F, Rossi M, Brozzetti S,
15 Masciangelo R, Passariello R, Catalano C. Intraindividual comparison of
16 gadoxetate disodium-enhanced MR imaging and 64-section multidetector CT in the
17 Detection of hepatocellular carcinoma in patients with cirrhosis. *Radiology*. 2010;
18 256:806-16.

- 1 16. Hidaka M, Eguchi S, Okudaira S, Takatsuki M, Tokai H, Soyama A, Nagayoshi S,
2 Mochizuki S, Hamasaki K, Tajima Y, Kanematsu T. Multicentric occurrence and
3 spread of hepatocellular carcinoma in whole explanted end-stage liver. *Hepatol Res.*
4 2009; 39:143-8.
- 5 17. Mazzaferro V, Regalia E, Doci R, Andreola S, Pulvirenti A, Bozzetti F, Montalto F,
6 Ammatuna M, Morabito A, Gennari L. Liver transplantation for the treatment of
7 small hepatocellular carcinomas in patients with cirrhosis. *N Engl J Med.* 1996;
8 334:693-9.
- 9 18. Eguchi S, Takatsuki M, Hidaka M, Tajima Y, Kanematsu T. Evolution of living
10 donor liver transplantation over 10 years: experience of a single center. *Surg Today.*
11 2008; 38:795-800.
- 12 19. International Consensus Group for Hepatocellular Neoplasia. Pathologic diagnosis
13 of early hepatocellular carcinoma: a report of the international consensus group for
14 hepatocellular neoplasia. *Hepatology.* 2009; 49:658-664.
- 15 20. Motosugi U, Ichikawa T, Sou H, Sano K, Tominaga L, Kitamura T, Araki T. Liver
16 parenchymal enhancement of hepatocyte-phase images in
17 Gd-EOB-DTPA-enhanced MR imaging: which biological markers of the liver
18 function affect the enhancement? *J Magn Reson Imaging.* 2009; 30:1042-1046.

- 1 21. Tajima T, Takao H, Akai H, Kiryu S, Imamura H, Watanabe Y, Shibahara J, Kokudo
2 N, Akahane M, Ohtomo K. Relationship between liver function and liver signal
3 intensity in hepatobiliary phase of gadolinium ethoxybenzyl diethylenetriamine
4 pentaacetic acid-enhanced magnetic resonance imaging. *J Comput Assist Tomogr.*
5 2010; 34:362-6.
- 6 22. Mita K, Kim SR, Kudo M, Imoto S, Nakajima T, Ando K, Fukuda K, Matsuoka T,
7 Maekawa Y, Hayashi Y. Diagnostic sensitivity of imaging modalities for
8 hepatocellular carcinoma smaller than 2 cm. *World J Gastroenterol.* 2010;
9 16:4187-92.
- 10 23. Kitao A, Matsui O, Yoneda N, Kozaka K, Shinmura R, Koda W, Kobayashi S,
11 Gabata T, Zen Y, Yamashita T, Kaneko S, Nakanuma Y. The uptake transporter
12 OATP8 expression decreases during multistep hepatocarcinogenesis: correlation
13 with gadoxetic acid enhanced MR imaging. *Eur Radiol.* 2011; 21:2056-66.
- 14 24. Ma M, Sakamoto M, Yamazaki K, Ohta T, Ohki M, Asaka M, Hirohashi S.
15 Expression profiling in multistage hepatocarcinogenesis: identification of HSP70 as
16 a molecular marker of early hepatocellular carcinoma. *Hepatology.* 2003;
17 37:198-207.
- 18 25. Stefaniuk P, Cianciara J, Wiercinska-Drapalo A. Present and future possibilities for

- 1 early diagnosis of hepatocellular carcinoma. *World J Gastroenterol.* 2010;
- 2 16:418-24.
- 3
- 4

1 Figure Legends

2 Figure 1. The expression of OATP2/OATP8 in liver parenchyma and HCC

3 Figure 2. Undetectable HCC in dysplastic nodule, well differentiated, 8mm

4 Figure 3. No expression of OATP is shown in A, B. Weak expression is shown in C, D

5

6

Table 1. Accuracy, Sensitivity and Positive predictive value of MD-CT, Gd-EOB-MRI

	MD-CT	Gd-EOB-MRI	p-value
Accuracy	53.5% (15/28)	57.1% (16/28)	N.S.
Sensitivity	55.5% (15/27)	59.2% (16/27)	N.S.
Positive predictive rate	88.2% (15/17)	94.1% (16/17)	N.S.

Table 2. The characteristics of detectable and undetectable HCC in the explanted liver

	detectable HCC (n=16)	undetectable HCC (n=11)	p-value
MD-CT			
hypervascular	86.7% (13/15)		
wash out	33.3% (5/15)		
Gd-EOB-MRI			
hypervascular	81.3% (13/16)		
hypointense (hepatobiliary phase)	68.8% (11/16)		
diameter (cm)	1.85 (0.7 - 4.2)	0.8 (0.2 - 1.1)	<0.001
Differentiation			
Well	13	9	0.97
Moderate	3	2	

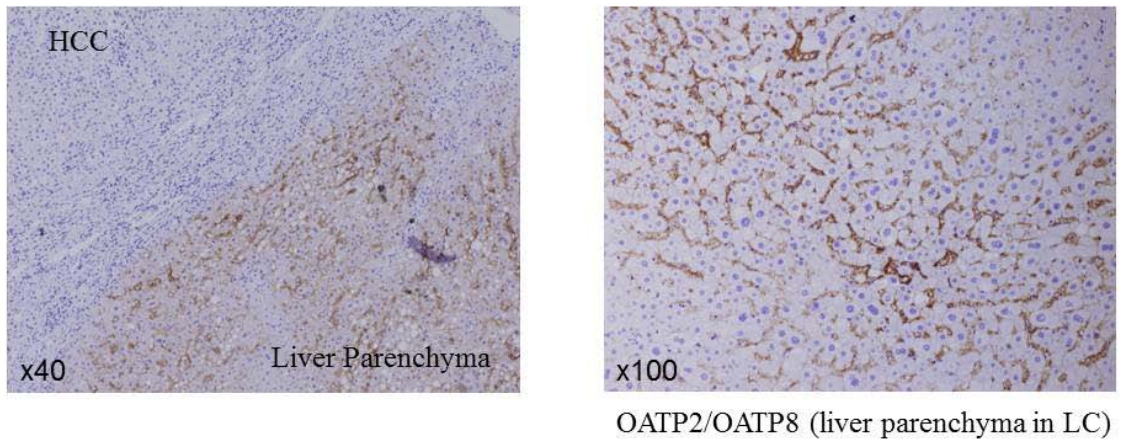


Figure 1. The expression of OATP2/OATP8 in liver parenchyma and HCC

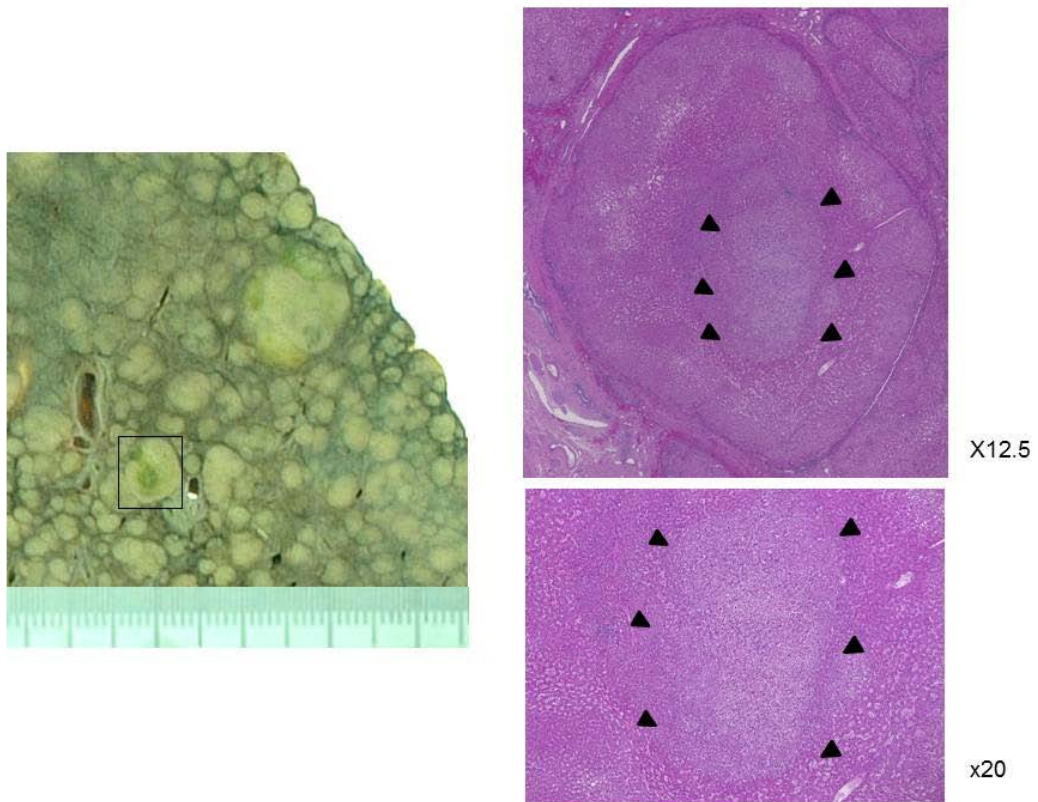


Figure 2. An undetectable HCC by Gd-EOB-MRI, well differentiated, 8 mm in a dysplastic nodule

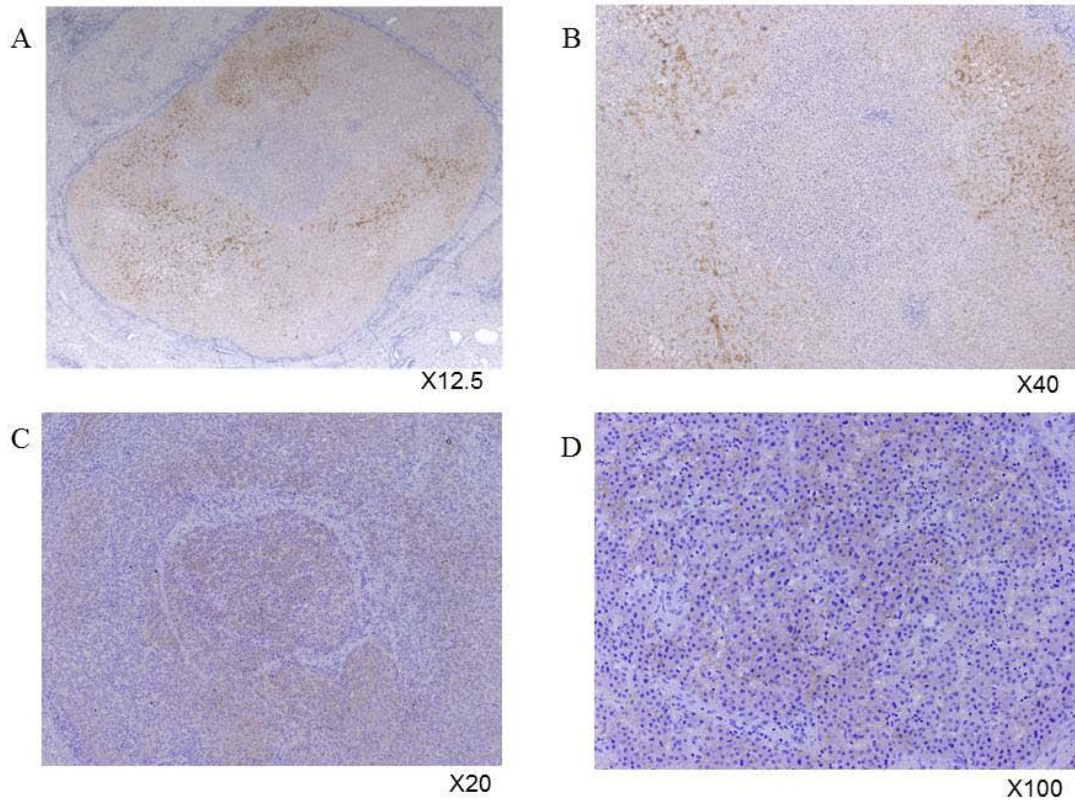


Figure 3. The lack of expression of OATP in undetectable HCC by Gd-EOB-MRI in A and B. Weak expression is shown in C and D.